

# Generation of Paired Photons with Controllable Waveforms

Vlatko Balić,\* Danielle A. Braje, Pavel Kolchin, G. Y. Yin, and S. E. Harris  
*Edward L. Ginzton Laboratory, Stanford University, Stanford, California 94305*  
 (Dated: February 23, 2005)

We describe experiments and theory showing the generation of counterpropagating paired photons with coherence times of about 50 ns and waveforms that are electronically controllable. Using cw lasers, electromagnetically induced transparency (EIT) and cold  $^{87}\text{Rb}$  atoms we generate paired photons into opposing single mode optical fibers at a rate of  $\sim 12000$  pairs per second.

PACS numbers: 42.50.Gy,32.80.-t,42.65.Lm,42.50.Dv,03.67.-a

Spontaneous parametric down-conversion in nonlinear crystals has become the near-standard method for generating correlated and entangled photon pairs [1]. These paired photons are routinely used in areas such as quantum measurement, imaging, and information transfer [2]. The existing sources of paired photons have limitations for certain applications: a) their linewidth is too broad, and their spectral brightness is too low to allow excitation of atomic species; b) because their coherence time is in the sub-picosecond range, photon waveforms are not resolvable by existing photodetectors; and c) their short coherence length,  $\sim 100 \mu\text{m}$ , is prohibitively small for long distance quantum communication.

In this Letter, following the field-opening papers of the Lukin [3] and Kimble [4] groups, we describe a source of paired photons that decisively overcomes the aforementioned limitations. This source makes use of slow light with a variable group velocity thereby allowing the control of the width, and to some extent, of the shape of the quantum wavepacket. We describe experimental results showing the generation of paired photons into opposing single mode fibers at a rate of 12000 pairs per second with a controllable wavepacket width in the range of 50 ns.

To motivate what follows, we first consider an ideal non-degenerate parametric down converter where pump photons are spontaneously converted to signal and idler photons and where the signal propagates with a group velocity  $V_g$  that is much slower than that of the idler. Figure 1 shows the analytical solution for the normalized intensity correlation function  $g^{(2)}$  of the signal with the idler. Because paired signal and idler photons have equal probability of being generated anywhere in the crystal of length  $L$ , the correlation function is rectangular with a temporal width that is equal to the group delay time  $L/V_g$ . With  $R$  defined as the paired generation rate (photons / second), the height of the correlation function is  $V_g/(RL)$  and is equal to the ratio of the average time between emitted photons to the length of the photon wavepacket of a single pair of photons. If the group velocity is varied, the width and height of  $g^{(2)}$  vary accordingly. The two-photon waveform is determined by  $g^{(2)}$ . For example, if the paired photons are used in a sum frequency experiment and are focused to an area  $A$ , the power per area of both photons is determined by the length of the generating crystal and is  $\hbar\omega V_g/(LA)$ .

The seminal paper by Duan *et al.* [5] described the entanglement of distant atomic ensembles and thereby motivated the search for methods for generating narrow-band correlated photons. Working with hot atoms and forward waves, van der Wal *et al.* have demonstrated both atomic memory and correlation between classical fields [3]. Kuzmich *et al.* have used the detected Stokes photon to time the generation of an anti-Stokes photon, thereby generating

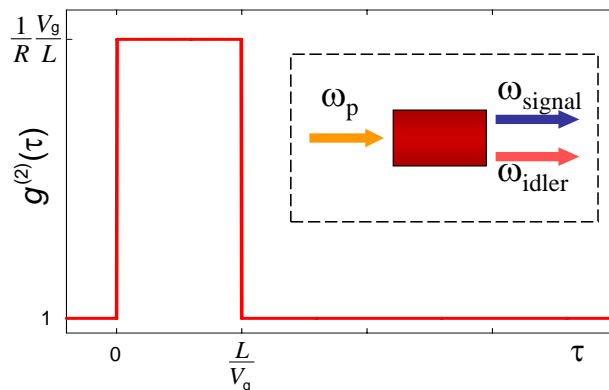


FIG. 1: Intensity correlation function for a spontaneous down converter with a length  $L$ , relative group delay  $V_g$  and paired emission rate  $R$ .

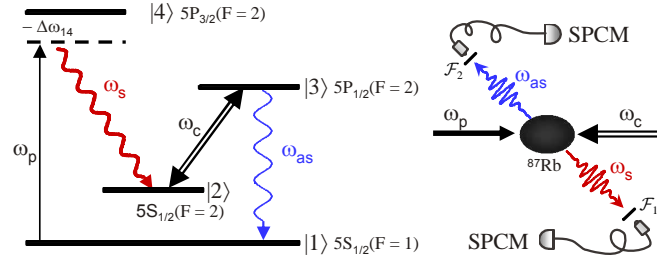


FIG. 2: Energy level diagram and schematic for spontaneous backward-wave paired photon generation in cold  $^{87}\text{Rb}$  atoms. In the presence of strong pump and coupling lasers, phase-matched, counterpropagating Stokes and anti-Stokes photons are generated into single mode fibers and detected by single photon counting modules (SPCM). Filters  $\mathcal{F}_1$  and  $\mathcal{F}_2$  are narrow-band interference filters at 780 nm and 795 nm, respectively.

non-classical photon pairs [4]. Braje *et al.* have used the same experimental setup described here and have reported EIT-based classical field backward-wave generation [6]. Further connections to earlier work include: the demonstration of interference of quantum wave packets [7], the effect of dispersion on these wavepackets [8], the suggestion for the use of EIT for nonlinear optical processes [9], the observation of slow light [10], experiments by Scully and colleagues on a backward-wave EIT process, and theoretical studies of photon correlation [11]. Recently, Chou *et al.* and Eisaman *et al.* have demonstrated single photon generation [12] and shaped few-photon light pulses [13].

Figure 2 shows a schematic of the process considered here. In the presence of two counterpropagating cw pump and coupling lasers with angular frequencies  $\omega_p$  and  $\omega_c$ , paired spontaneous Stokes and anti-Stokes photons are generated and propagate in opposite directions. These frequencies satisfy  $\omega_s + \omega_{as} = \omega_p + \omega_c$ . The wavelengths of the Stokes and anti-Stokes photons are 780 nm and 795 nm, respectively. The anti-Stokes photon has a center frequency equal to that of the highly absorbing  $|1\rangle \rightarrow |3\rangle$  transition. The coupling laser creates a transparency window and causes the anti-Stokes wave to travel at a slow and variable group velocity  $V_g$ . This group velocity determines the width of the paired photon wavepacket. The dominant process of Fig. 2 is the phase-matched backward-wave parametric interaction between the Stokes and anti-Stokes waves. The complexity of this interaction is increased by the presence of Raman gain and scattering at the Stokes frequency and by EIT and slow light at the anti-Stokes frequency.

Working in the Heisenberg picture, the slowly varying envelope equations for the frequency domain operators  $a_s^\dagger(-\omega)$  and  $a_{as}(\omega)$  are:

$$\begin{aligned} \frac{\partial a_s^\dagger}{\partial z} + g_R a_s^\dagger + \kappa_s a_{as} &= F_s \\ - \frac{\partial a_{as}}{\partial z} + \Gamma a_{as} + \kappa_{as} a_s^\dagger &= F_{as}, \end{aligned} \quad (1)$$

where  $F_s = \xi_s f_{12} + \eta_s f_{13}$  and  $F_{as} = \xi_{as} f_{12} + \eta_{as} f_{13}$  are the commutator preserving Langevin operators and  $\langle f_{ij}(\omega, z) f_{ij}^\dagger(\omega', z') \rangle = (1/2\pi) \delta(\omega - \omega') \delta(z - z')$ . In Eq. (1),  $\Gamma(\omega)$  is the EIT profile,  $g_R(\omega)$  is the (complex) Raman gain, and  $\kappa_s(\omega)$  and  $\kappa_{as}(\omega)$  are the parametric coupling constants. We calculate these coefficients using the assumption that the atomic population remains in the ground state. With  $\omega$  as the detuning of the anti-Stokes frequency from the  $|1\rangle \rightarrow |3\rangle$  transition,  $\Delta\omega_{14}$  as the detuning of the pump laser from  $|1\rangle \rightarrow |4\rangle$  transition, dephasing rates  $\gamma_{12}$  and  $\gamma_{13}$ , atom density  $N$ , an absorption cross section  $\sigma$  for all allowed transitions, and the definitions  $\tilde{\omega}_{12} = \omega + i\gamma_{12}$ ,  $\tilde{\omega}_{13} = \omega + i\gamma_{13}$ , and  $D(\omega) = |\Omega_c|^2 - 4\tilde{\omega}_{12}\tilde{\omega}_{13}$ , the quantities in Eq. (1) are:

$$\begin{aligned} \Gamma &= -\frac{2iN\sigma\gamma_{13}\tilde{\omega}_{12}}{D(\omega)}, \quad g_R = -\left(\frac{\Omega_p^2\tilde{\omega}_{13}}{4\Delta\omega_{14}^2\tilde{\omega}_{12}}\right)\Gamma, \\ \kappa_s &= -\kappa_{as} = \left(\frac{\Omega_p}{2\Delta\omega_{14}}\right)\frac{iN\sigma\gamma_{13}\Omega_c}{D(\omega)}, \\ \xi_s &= \left(\frac{\Omega_p}{\Delta\omega_{14}}\right)\frac{2\tilde{\omega}_{13}\sqrt{N\sigma\gamma_{13}\gamma_{12}}}{D(\omega)}, \\ \eta_s &= -\left(\frac{\Omega_c}{2\tilde{\omega}_{13}}\right)\sqrt{\frac{\gamma_{13}}{\gamma_{12}}}\xi_s, \end{aligned}$$

$$\xi_{as} = -\frac{2\Omega_c\sqrt{N\sigma\gamma_{13}\gamma_{12}}}{D(\omega)},$$

$$\eta_{as} = -\sqrt{\frac{\gamma_{13}}{\gamma_{12}}}\left(\frac{2\tilde{\omega}_{12}}{\Omega_c}\right)\xi_{as}. \quad (2)$$

We first estimate the expected rate of paired counts by setting the Langevin terms in Eq. (1) equal to zero, neglecting the Raman term  $g_R$ , and assuming that the optical depth  $N\sigma L$  is sufficiently large such that the anti-Stokes counts are generated near the line center of the EIT profile. When this is the case, we may approximate the EIT profile as  $\Gamma(\omega) = -i\omega/V_g$ . The solution of Eq. (1) is then written as a linear combination of the boundary conditions  $a_s^\dagger(z=0)$  and  $a_{as}^\dagger(z=L)$ . The quantities of interest, both here and later, are obtained as expected values of product (boundary) vacuum states. The single transverse mode spectral generation rate  $S(\omega)$  and the spectrally integrated generation rate  $S = \frac{1}{2\pi} \int S(\omega)d\omega$  are:

$$S(\omega) = |\kappa|^2 L^2 \text{sinc}^2\left(\frac{\omega L}{2V_g}\right)$$

$$S = V_g |\kappa|^2 L. \quad (3)$$

The group velocity of the anti-Stokes wave is  $V_g = \Omega_c^2/(2\gamma_{13}N\sigma)$ . Using typical values for the parameters:  $\gamma_{13} = 1.8 \cdot 10^7 \text{ s}^{-1}$ ,  $N = 8 \times 10^{10} \text{ atoms cm}^{-3}$ ,  $\sigma = 10^{-9} \text{ cm}^2$ ,  $L = 1.5 \text{ mm}$ , and  $\Omega_c = 8\gamma_{13}$  yields  $V_g = c/3500$ ,  $|\kappa| = 45 \text{ m}^{-1}$  and a paired count rate of about  $2.6 \times 10^5$  pairs per second. At an optical depth of  $N\sigma L = 10$ , Eq. (3) predicts generation rates that are about twice as large as those obtained by numerical solution of Eq. (1). At higher optical depths, Eq. (3) becomes increasingly accurate.

Analogous to parametric down-conversion in crystals, the spectral generation rate  $S(\omega)$  scales as  $(NL)^2$ , while the total rate of paired counts scales linearly as  $NL$ . The Langevin noise terms in Eq. (1) result in additional unpaired Stokes and anti-Stokes counts both of which vary linearly with  $NL$ .

Paired photon generation is achieved in a gas of cold  $^{87}\text{Rb}$  atoms which are cooled and trapped in a dark magneto-optical trap in the  $5S_{1/2}(F=1)$  level [6]. The optical depth  $N\sigma L$  is varied from 1 to 11 by changing the detuning of the trapping laser from  $5P_{3/2}(F'=3)$  level. The photon-counting experiment is performed in the presence of the trapping, magnetic quadrupole field in a  $500 \mu\text{s}$  window  $10 \mu\text{s}$  after shutting off the trapping beams. By turning on the trapping and repumping lasers before the cold atoms have expanded out of the trapping region, the atom cloud is quickly recycled. This procedure allows a duty cycle (experimental time to trapping time) of up to 30%. EIT is obtained at the anti-Stokes wavelength by using pump and coupling lasers with opposite circular polarizations.

The pump laser is frequency stabilized  $7.5 \gamma_{13}$  below the  $5S_{1/2}(F=1) \rightarrow 5P_{3/2}(F'=2)$  transition of  $^{87}\text{Rb}$ . The 680 nW laser is focused to a  $1/e^2$  diameter of  $280 \mu\text{m}$  with a Rabi frequency of  $\Omega_p = 0.8 \gamma_{13}$ . The coupling laser, locked on the  $5S_{1/2}(F=2) \rightarrow 5P_{1/2}(F'=2)$  transition, has a  $1/e^2$  diameter of  $950 \mu\text{m}$  in the atom cloud with a Rabi frequency variable from 4 to  $30 \gamma_{13}$ .

As shown in Fig. 2, anti-Stokes and Stokes photons are counterpropagating through two single-mode fibers separated by 0.8 m. These fibers are aligned to each other through the atom cloud with a measured fiber-coupling efficiency of 80%. We choose the angle between the Stokes/anti-Stokes axis and the axis defined by the pump and coupling lasers to be  $\sim 2^\circ$  which provides spatial separation between the weak anti-Stokes and Stokes photons from the two strong beams. Because the Stokes and anti-Stokes waves have different frequencies, it is not possible to have exact phase matching in the backward-wave configuration. The phase-matching of these lasers is discussed in detail in our earlier work [6]. Narrow-band, interference filters ( $\mathcal{F}_1$  at 780 nm for Stokes fiber and  $\mathcal{F}_2$  at 795 nm for anti-Stokes fiber) are used to reduce the uncorrelated noise. The single-mode fibers are connected to photon counting modules (Perkin-Elmer SPCM-AQR-13). A time-to-digital converter (Fast Comtec 7886S) measures the time between each ‘‘start’’ Stokes photon and ‘‘stop’’ anti-Stokes photon. Correlation statistics are binned into 128-bin histograms with bin-width of 1 ns.

We turn now to the main work of this Letter: the discussion and measurement of the shape of the (non-normalized) Glauber two-photon correlation function:

$$G^{(2)}(\tau) = \langle a_s^\dagger(t)a_{as}^\dagger(t+\tau)a_{as}(t+\tau)a_s(t) \rangle. \quad (4)$$

The shape of  $G^{(2)}(\tau)$  is expected to depend on the relation of two characteristic times that are the essence of this problem. The first of these times is a Rabi-like time  $t_r = 1/\sqrt{\Omega_c^2 - \gamma_{13}^2}$  and the second is the group delay time of the medium  $t_g = L/V_g$ .

When  $t_g < t_r$  and  $\Omega_c > \gamma_{13}$  then  $G^{(2)}(\tau)$  is oscillatory and damped [14]. The experimental results in this regime are shown in Fig. 3. One observes behavior like a single atom, where at  $t=0$  a Stokes photon causes the excitation of

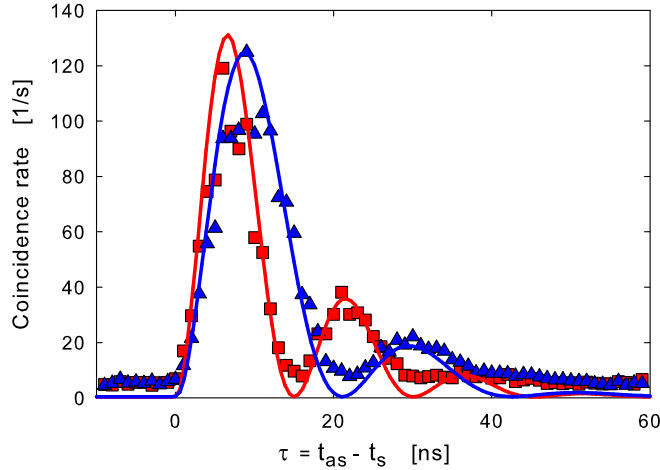


FIG. 3: Correlation function in the oscillatory regime. Coincidence rate  $R_c(\tau)$  as a function of the time difference between the detection of anti-Stokes and Stokes photons as shown for  $\Omega_c = 23.4 \gamma_{13}$  ( $\square$ ) and  $\Omega_c = 16.8 \gamma_{13}$  ( $\triangle$ ), all with  $N\sigma L = 11$ . Data was collected over 200 s with duty cycle of 10%, and a bin size of 1 ns. Theoretical curves (solid lines) are scaled vertically with no additional free parameters.

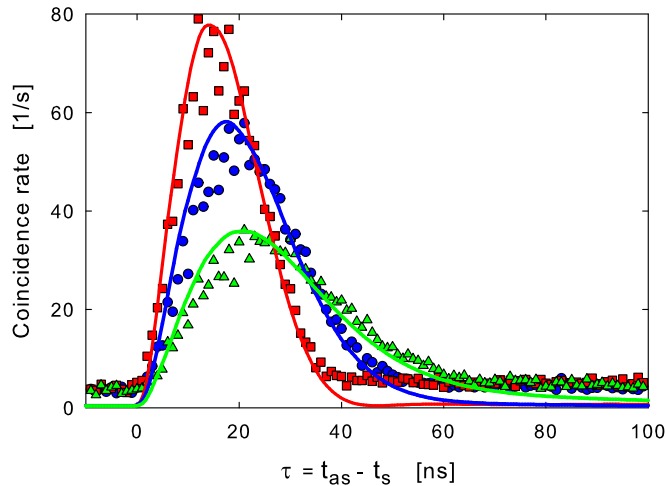


FIG. 4: Correlation function in the group delay regime. Coincidence rate  $R_c(\tau)$  as a function of the time difference between the detection of anti-Stokes and Stokes photons as shown for  $\Omega_c = 8.4 \gamma_{13}$  ( $\square$ ),  $\Omega_c = 6.0 \gamma_{13}$  ( $\bullet$ ), and  $\Omega_c = 4.0 \gamma_{13}$  ( $\triangle$ ), all with  $N\sigma L = 11$ . Data was collected over 200 s and bin size is 1 ns. Theoretical curves are vertically scaled.

state  $|2\rangle$ , and the probability amplitude oscillates between states  $|2\rangle$  and  $|3\rangle$  as the atom decays. In Fig. 3 the optical depth is fixed at  $N\sigma L = 11$  and  $\Omega_c$  is varied. The squares and triangles are the coincidence rates  $R_c(\tau)$  acquired over 200 seconds and corrected for the 10% duty cycle. Statistical uncertainty of the peak coincidence rates is less than 3%. The theoretical curves (solid lines) are obtained by numerically solving Eq. (1) with all terms retained and evaluating the quantity given in Eq. (4). The parameters for the theoretical curves are  $N\sigma L = 11$ ,  $\Omega_p = 0.8 \gamma_{13}$ ,  $\Delta\omega_{14} = 7.5 \gamma_{13}$ . Each of the theoretical curves is vertically scaled to the experimental data with no additional free parameters.

When the group delay is sufficiently large such that  $t_r < t_g$ ,  $G^{(2)}(\tau)$  approximates the correlation function of the ideal parametric emitter of Fig. 1, and the width of the wavepacket is approximately  $t_g$ . Figure 4 shows experiment and theory in this limit where the correlation width is set by the variable group velocity. As in Fig. 3, the optical depth is fixed at  $N\sigma L = 11$ , and the group velocity is varied by changing the coupling laser Rabi frequency. In the first experimental curve (squares), corresponding to  $\Omega_c = 8.4 \gamma_{13}$ , the width of the correlation function is  $\sim 20$  ns. By

increasing the group delay, which is inversely proportional to the group velocity, the peak height of the coincidence curve decreases; this trend can be seen in the subsequent data curves. As earlier, the theoretical curves are vertically scaled to the experimental data with no additional free parameters.

In any EIT process whether with classical light or with single photons as observed here, the maximum group delay that may be observed is limited by linewidth of the  $|1\rangle \rightarrow |2\rangle$  transition [15]. Here, we estimate this linewidth from a least-squares fit of the observed EIT profiles at small coupling Rabi frequency. This yields an effective dephasing rate of  $\gamma_{12} = 0.6 \gamma_{13}$ . The maximum delay and thus the maximum paired photon pulse width is therefore  $1/(2\gamma_{12}) = 45$  ns. This maximum delay is in reasonable agreement with the  $\Omega_c = 4.0 \gamma_{13}$  curve of Fig. 4.

We next compare the experimental results and the predictions of Eq. (1). First, as noted above, the agreement between theory and experiment describing the shapes of the non-normalized  $G^{(2)}(\tau)$  is excellent over our parameter range. The generation rate for our paired counts is estimated from correlation curves by subtracting the uncorrelated flat background and measuring the area. Taking into account detection efficiencies, we typically generate paired photons at a rate of  $\sim 12000 \text{ s}^{-1}$ , which is low as compared to theory by a factor of about 10. Also, the measured conversion efficiency between a weak input Stokes beam and the generated anti-Stokes beam is low by this same factor. We believe that this discrepancy is the result of our use of focused (non-planar) pump and coupling laser beams which were focused to reduce scatter background. A much more important discrepancy is the experimental finding that the observed anti-Stokes rate is nominally equal to the observed Stokes rate. It appears that our anti-Stokes counts are of two types: paired counts that occur with a delay of less than  $\sim 50$  ns (Figs. 3 and 4) and non-paired counts that occur over much longer times. The observed ratio of unpaired to paired counts is  $\sim 15$ . We suspect, but have no direct evidence, that the unpaired anti-Stokes counts result from the dephased  $|1\rangle \rightarrow |2\rangle$  transitions atoms that must ultimately return to the ground level if the system is to remain in steady state.

When the bin-width  $\Delta T$  is small as compared to the temporal correlation time,  $G^{(2)}$  is related to the measured coincidence rates of Figs. 3 or 4 by  $G^{(2)}(\tau) \approx R_c(\tau)/(\epsilon^2 \Delta T)$ . In this experiment  $\Delta T = 1$  ns, and the efficiency factor  $\epsilon = 0.3$ . This efficiency factor accounts for the photon counter efficiency of 50%, the filter transmission of 75%, and the fiber coupling efficiency of 80%. With  $R_s$  and  $R_{as}$  defined as the similarly corrected Stokes and anti-Stokes rates, the normalized intensity correlation function is then  $g^{(2)}(\tau) = G^{(2)}(\tau)/(R_s R_{as})$ . We thereby estimate  $G^{(2)}(\tau) = 8 \times 10^{11} \text{ s}^{-2}$  and for  $R_s = R_{as} = 180000 \text{ s}^{-1}$ ,  $g^{(2)}(\tau) = 25$ . For a classical light source, the cross-correlation is bounded by the product of auto-correlations as described by the Cauchy-Schwartz inequality [16]:  $[g_{s,as}^{(2)}(\tau)]^2 / (g_{s,s}^{(2)} \cdot g_{as,as}^{(2)}) \leq 1$ . For our paired photon source, this inequality is violated by a factor of  $\sim 400$ .

This work has described experiments and theory showing the generation of oppositely propagating paired photons with coherence times of  $\sim 50$  ns and waveforms that are electronically controllable. It is expected that these non-degenerate paired photons will exhibit time-frequency entanglement [17]. Operation with oppositely polarized pump and coupling laser beams, will result in polarization entanglement of the paired photons. By using the same transition and detuning the pumping laser, the frequencies of the Stokes and anti-Stokes photons may be made the same. Because they are narrow band, paired photons that are generated by this technique should be useful for transferring correlated and entangled momenta to cold atoms [18].

The authors thank A. Andre, M. Lukin, E. Waks and Y. Yamamoto for helpful discussions. We thank W. E. Moerner and R. Zare for help with coincidence counting equipment which was crucial to the experiment, and M. Scully for suggesting the Rabi flopping generation regime. The work was supported by the the Defense Advanced Research Projects Agency, the U.S. Air Force Office of Scientific Research, the U.S. Army Research Office, and the Multidisciplinary Research Initiative Program.

---

\* Electronic address: [vbalic@stanford.edu](mailto:vbalic@stanford.edu)

- [1] S. E. Harris, M. K. Oshman, and R. L. Byer, *Phys. Rev. Lett.* **18** 732 (1967); D. Burnham and D. Weinberg, *Phys. Rev. Lett.* **25**, 84 (1970).
- [2] D. Bouwmeester, A. Ekert, A. Zeilinger, *The Physics of Quantum Information* (Springer-Verlag, Berlin, 2000).
- [3] C. H. van der Wal, M. D. Eisaman, A. Andre, R. L. Walsworth, D. F. Phillips, A. S. Zibrov, and M. D. Lukin, *Science* **301**, 196 (2003).
- [4] A. Kuzmich, W. P. Bowen, A. D. Boozer, A. Boca, C. W. Chou, L. M. Duan, and H. J. Kimble, *Nature* **423**, 731 (2003).
- [5] L. M. Duan, M. D. Lukin, J. I. Cirac, and P. Zoller, *Nature* **414**, 413 (2001).
- [6] D. A. Braje, V. Balić, S. Goda, G. Y. Yin, and S. E. Harris, *Phys. Rev. Lett.* **93**, 183601 (2004).
- [7] M. Atature, A. V. Sergienko, B. E. A. Saleh, and M. C. Teich, *Phys. Rev. Lett.* **86**, 4013 (2001).
- [8] A. Valencia, M. V. Chekhova, A. Trifonov, and Y. Shih, *Phys. Rev. Lett.* **88**, 183601 (2002).
- [9] S. E. Harris, J. E. Field, and A. Imamoglu, *Phys. Rev. Lett.* **64**, 1107 (1990).

- [10] L. V. Hau, S. E. Harris, Z. Dutton, and C. H. Behroozi, *Nature* **397**, 594 (1999).
- [11] M. D. Lukin, A. B. Matsko, M. Fleischhauer, and M. O. Scully, *Phys. Rev. Lett.* **82**, 1847 (1999). A. S. Zibrov, M. D. Lukin, and M. O. Scully, *Phys. Rev. Lett.* **83**, 4049 (1999).
- [12] C. W. Chou, S. V. Polyakov, A. Kuzmich, and H. J. Kimble, *Phys. Rev. Lett.* **92**, 213601 (2004). S. V. Polyakov, C. W. Chou, D. Felinto, and H. J. Kimble, *Phys. Rev. Lett.* **93**, 263601 (2004).
- [13] M. D. Eisaman, L. Childress, A. Andre, F. Massou, A. S. Zibrov, and M. D. Lukin, *Phys. Rev. Lett.* **93**, 233602 (2004).
- [14] M. O. Scully and C. H. R. Ooi, *J. Opt. B* **6**, S816 (2004).
- [15] S. E. Harris, J. E. Field, and A. Kasapi, *Phys. Rev. A* **46**, R29 (1992).
- [16] J. F. Clauser, *Phys. Rev. D* **9**, 853 (1972).
- [17] J. D. Franson, *Phys. Rev. Lett.* **62**, 2205 (1989).
- [18] P. D. Lett, *J. Mod. Opt.* **51**, 1817 (2004).

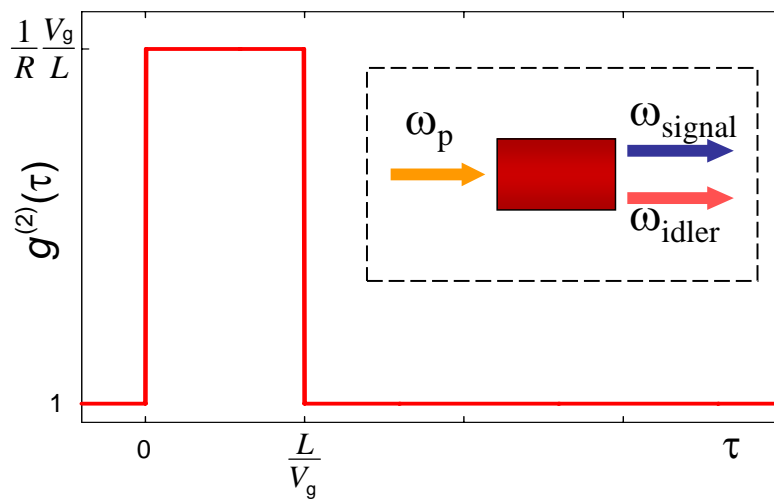


Figure 1